

Instrument Science Report WFPC2 2010-002

Improved WF4 Anomaly Corrections

V. Dixon and J. Biretta
June 29, 2010

ABSTRACT

The WF4 anomaly is a temperature-dependent reduction in the gain of the WF4 CCD. Software added to calwp2 corrects stellar photometry to ~ 0.01 magnitude, but undercorrects the CCD bias level by several DN. While tracking down this discrepancy, we discovered three other complications that motivated us to construct a new set of reference files: a discontinuity in the WF4 anomaly between pixels in the image and the overscan region, unexpected structure in the overscan region for low-bias images, and an error in the application of the reference file by calwp2. New reference files that correct for these effects have been created and used to reprocess all low-bias images in the WFPC2 static archive.

Introduction

Since early 2002, the WF4 detector of the Wide Field Planetary Camera 2 (WFPC2) has exhibited an anomaly characterized by low or zero bias levels, faint horizontal streaks, and low count levels (Biretta and Gonzaga 2005). To correct for its effects, a WF4 gain-correction step was added to the WFPC2 data-reduction pipeline (Dixon and Biretta 2009). Photometric tests using bright stars indicated that the corrected images are generally accurate to ~ 0.01 magnitude. The corrected bias levels, however, were lower than expected, which could lead to photometric problems for faint targets.

In Figures 1 and 2, we plot the corrected bias level, read from the BIASEVEN header keyword, as a function of the uncorrected bias level, read from the BIASEVNU keyword,

for a few thousand gain 7 and 15 images. In both figures, red points represent images processed with our initial calibration reference files, delivered in 2008. For the gain 7 images, the normal (pre-anomaly) bias level was 311 DN and ideally the bias would be corrected to this value, but the red points are 3-4 DN too low over most of the range. For the gain 15 images, the nominal bias level is 305 DN, but the red points scale linearly with the uncorrected bias. For example, when a bias value of 308 is subtracted from a corrected image for which the actual bias is 311, the entire image is three DN too bright. Such an error is insignificant for bright pixels, but for the faintest pixels in the image, the resulting error could be 100% or more, an important effect for faint, extended objects. Apparently our WF4 corrections have a small multiplicative error which primarily effects faint pixels in the image.

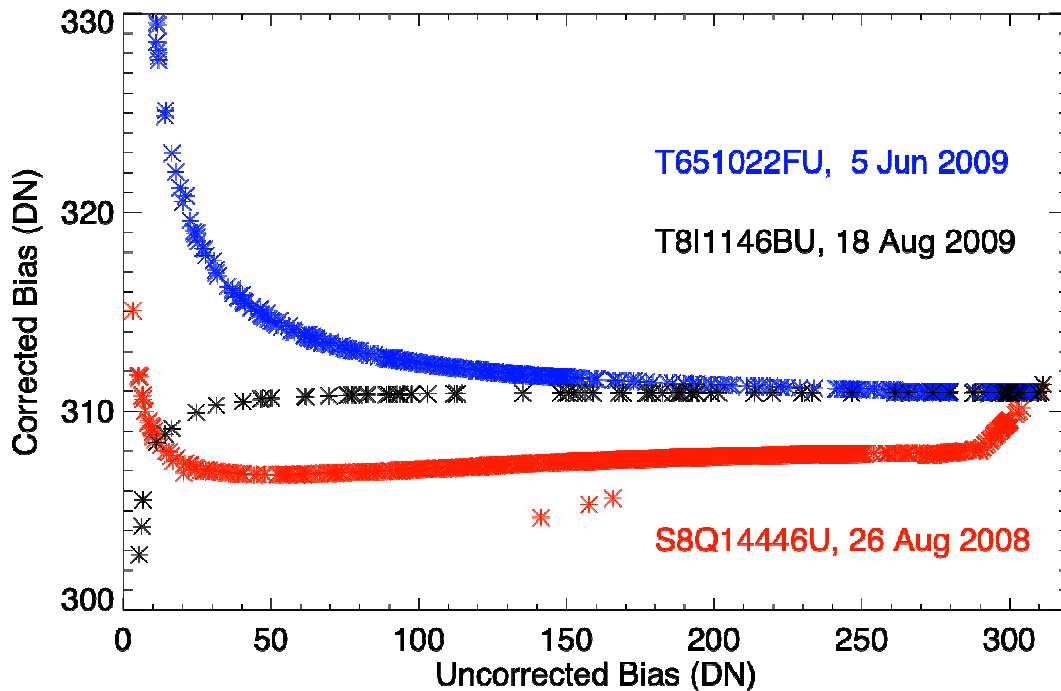


Figure 1. The corrected bias level (BIASEVEN) as a function of the uncorrected bias (BIASEVNU) for a set of WFPC2 images obtained with a gain of 7. The red points represent images processed with our initial calibration reference file. The blue points represent images processed with a revised file, for which the bias values were calculated by hand. The black points represent our final reference file, which corrects for an index error in calwp2. Ideally the corrected bias values would equal 311 DN, the normal value before onset of the WF4 anomaly, for all uncorrected bias values. The final reference file meets this condition except at the very lowest uncorrect bias values <40 DN.

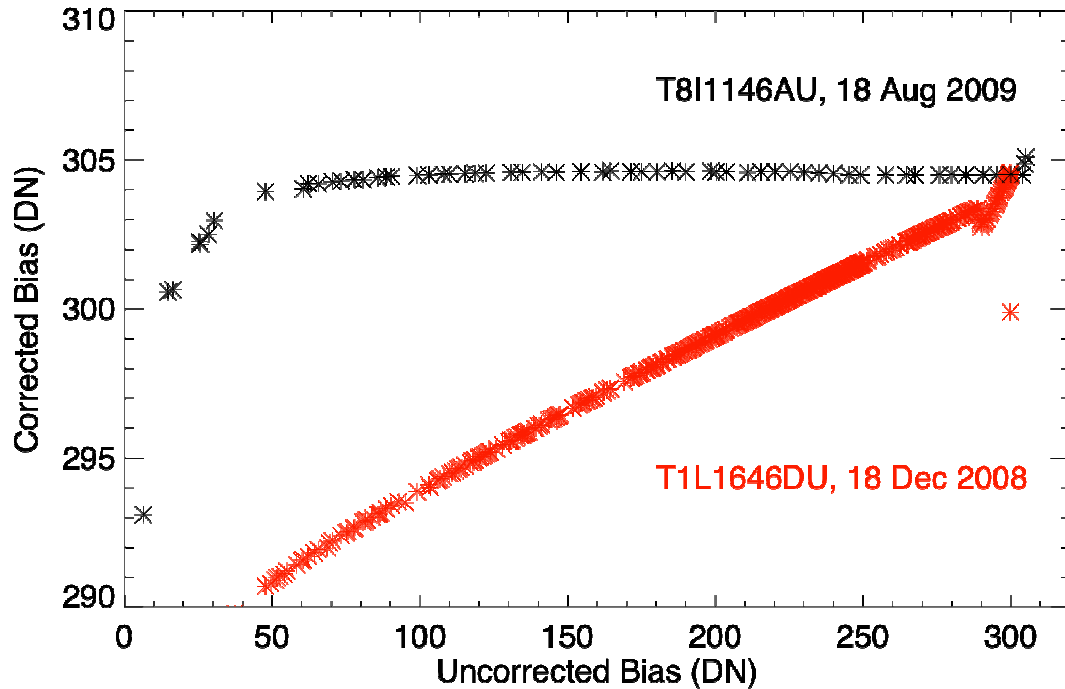


Figure 2. The corrected bias level (BIASEVEN) as a function of the uncorrected bias (BIASEVNU) for a set of WFPC2 images obtained with a gain of 15. The red points represent images processed with our initial calibration reference file. The black points represent our final reference file, which corrects for an index error in calwp2. Ideally the corrected bias values would always equal ~ 305 DN.

While tracking down this discrepancy, we discovered three other complications that motivated us to construct a new set of reference files: a discontinuity in the WF4 anomaly between pixels in the image and the overscan region, unexpected structure in the overscan region for low-bias images, and an error in the application of the correction by calwp2. We discuss these effects in the following three sections.

A Discontinuity in the WF4 Anomaly

The WF4 anomaly reduces the detector gain in a way that causes bright pixels to become a little fainter and faint pixels to become a lot fainter. WFPC2 pixel values range from 0 to 4095 DN. Over most of this range, the ratio of observed-to-actual intensity varies smoothly. In Figure 3, we plot this ratio for ten low-bias images. The green points were computed by identifying all pixels in a high-bias reference image with DN values 312.5—313.5, 313.5—314.5, etc., and computing their mean. (There are no fainter pixels. The right-most bin is 32 DN wide.) At each DN level, the same pixels are identified on a set of low-bias images and their mean computed. The ratio of the observed and reference DN levels is plotted as a function of the reference level. Only the inner 500×500 pixels of each chip are considered. The data are flat-field images obtained through the FR868N18 filter

with bias values ranging from 4 to 96 DN. The blue points were computed from the overscan regions of each image and represent our best estimate of their bias levels.

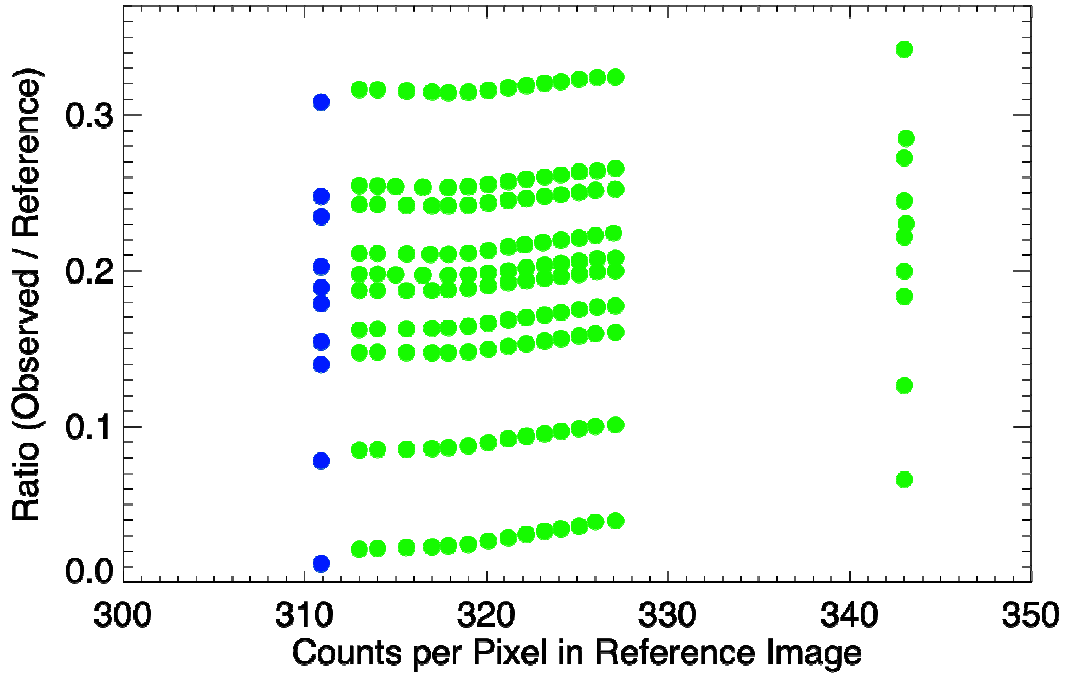


Figure 3. The ratio (observed mean) / (reference mean) as a function of the counts per pixel in the reference image for a set of gain 7 flat-field images. Uncorrected bias levels range from 4 to 96 DN. Blue points are computed from the overscan regions; green points from the inner 500x500 pixels of the WF4 chip.

The green points with reference values above ~ 320 DN form a line whose extrapolation to low DN values intersects the blue points. The green points with reference values below 320 flatten out, and there is a discontinuity between the green points and the blue ones, that is, between the faintest image pixels and the overscan region. Because the actual distribution of pixel values extends from the green to the blue points (and on to lower DN values), we need a correction file whose values vary smoothly across the entire range. For the 2008 reference files, we decided to ignore the blue points and base our correction entirely on the green ones, fitting a curve to the faintest green points and extrapolating to lower DN values. As a result, for a given bias value, the overscan region was undercorrected for the WF4 anomaly and the corrected bias values written to the file header were too low.

To address this problem, we generated a second set of reference files, this time including the ratios derived from the overscan region (blue points), but excluding those from the image (green points) with $DN < 328$. We interpolated linearly between the blue points and the faintest remaining green ones (which are binned by 32 DN). The resulting reference file properly corrects the overscan region, but now overcorrects the faintest image pixels. Fortunately, the resulting errors are only a few percent, even for the faintest image pixels.

Persistence Effects in the Overscan Region

A second problem complicates our analysis of the WF4 anomaly. Figure 4 shows the distribution of counts in the overscan region of the WF4 image from observation u9kn130em, a flat-field image obtained through a linear-ramp filter. A slice of the image is also reproduced: it is bright at the bottom and becomes fainter with increasing Y . (Pixels with $Y < 45$ are shadowed by the pyramid, and in the overscan region these pixels are near the true bias level, which is about 59 DN.) We see that, where the image is bright, the bias level in the overscan region is depressed. The CCD is read out row by row, with the image and overscan pixels interleaved. At low bias levels, bright regions in the image trigger a negative persistence effect in the overscan region, reducing the observed counts. This could be attributed to a negative over-shoot of the CCD amplifier, when transitioning from bright image pixels to the dark overscan region, as the CCD row is readout. Where the CCD rows have only faint pixels (e.g., $Y > 600$ in Figure 4), the overscan region more accurately reflects the true bias level.

While real astrophysical images are seldom as bright as this flat-field image, fluctuations in the overscan region complicate our construction of a correction file for the WF4 anomaly. Calwp2 computes the image bias from pixels [8:13, 10:789] of the overscan region. (Here we use IDL notation, counting from 0.) The resulting bias of ~56 DN is clearly too low. We used calwp2 bias values in our original set of reference files, with the result that we applied the wrong correction to low-bias images. To better estimate the true image bias, we calculate it ourselves for these ramp filter flats, using pixels [8:13, 600:789]. An even more robust estimate might come from the shadowed region.

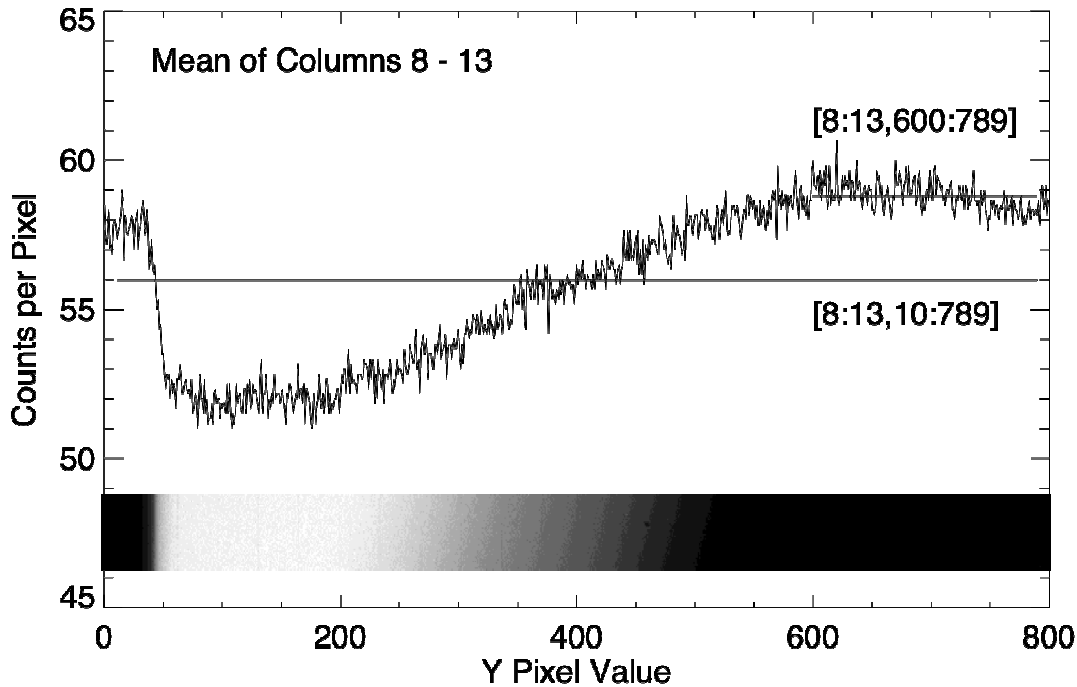


Figure 4. The overscan region of the WF4 image u9kn130em, a gain 7 flat-field image obtained through a linear-ramp filter. The mean value of columns 8 - 13 is plotted as a function of the Y-pixel value. Overplotted is a slice of the image [375:425, 0:799], which is brightest at small Y values (ignoring the pyramid mirror shadow at $Y < 50$) and fainter with increasing Y. At low bias levels, the overscan region suffers a negative persistence effect where the image is brightest.

An Indexing Error in Calwp2

Using revised bias estimates and ignoring image pixels with $DN < 328$, we constructed a second set of WF4 correction files. The results for several thousand gain 7 images are shown as blue points in Figure 1. For high-bias images, the correction is nearly perfect, but it diverges rapidly as the bias falls. Further investigation revealed an indexing error in calwp2. The WF4 reference files are constructed using IDL, which counts array elements from 0 to $N-1$. The pipeline is written in SPP, which counts array elements from 1 to N . The pipeline must thus increase the index value by 1 when extracting a row or column from the WF4 reference file. It does so when interpolating between bias values, but it neglects to do so when interpolating between individual DN values. That is, it extracts the correct row, but the wrong column. Rather than modifying the pipeline, we simply shifted the reference image by 1 column. Bias values corrected using the final set of reference files are plotted as black points in Figures 1 and 2. In both cases, the correction is accurate to within 1 DN for all bias levels above 50.

Reprocessing Low-Bias Files

By the time that these concerns were sorted out, final processing of the WFPC2 archive was nearly complete, and reprocessing all images taken since March of 2002 (and thus potentially affected by the WF4 anomaly) was impractical. Instead, we reprocessed only images whose corrected bias values were in error by more than 0.7%, corresponding to uncorrected bias values < 295 for gain 7 and < 270 for gain 15 data. All WFPC2 images in the MAST archive now have corrected bias values good to within 0.7%, except those with raw bias values < 50 , as shown in Figures 1 and 2.

Calwp2 sets a data-quality flag (2048 or bit number 11) for all pixels in images whose bias values are so low that they are unlikely to be properly corrected; this minimum bias value is read from the LOWBLEV keyword of the reference file. We have increased this value to 100 DN.

To check our results, we repeated the standard-star photometric tests discussed in Dixon and Biretta (2009). Our results are identical to that report and are not presented again here.

Conclusions

While investigating an error in the bias-level correction for the WF4 anomaly, we discovered two unexpected detector effects: an apparent discontinuity in the WF4 anomaly between the overscan region and the faintest pixels in the image, and structure in the overscan region due to persistence effects when the background is high and the bias is low. Finally, we identified an indexing error in calwp2. Modifying the WF4 correction files to account for these effects has improved the bias correction, reducing errors below 1 DN for bias levels above 50 DN. All WFPC2 images with bias errors greater than 0.7% have been reprocessed using the new reference files. Tests indicate that these changes have no effect on the photometry of moderately bright stars.

References

- Biretta, J. and Gonzaga, S. 2005, Early Assessment of the WF4 Anomaly (WFPC2 ISR 2005-02).
- Dixon, V. and Biretta, J. 2009, Pipeline Correction of Images Impacted by the WF4 Anomaly (WFPC2 ISR 2009-03).